A formulation for calculating the translational velocity of a vortex ring or pair

Kamran Mohseni

Department of Aerospace Engineering, University of Colorado, Boulder, CO 80309-429, USA

E-mail: mohseni@colorado.edu

Abstract
Cephalopods, among other marine animals, use jet propulsion for swimming. A simple
actuator is designed to loosely mimic pulsatile jet formation in squid and jellyfish. The
actuator is comprised of a cavity with an oscillating diaphragm and an exit orifice. Periodic
oscillation of the diaphragm results in the formation of an array of vortex rings and eventually
could generate a periodic pulsatile jet. A general formulation for calculating the velocity of a
steadily translating vortical structure in two-dimensional and axi-symmetric shear flows is
presented. This technique is based on taking the variational derivative of an energetic function
at its critical point. This technique is general, applicable to vortices in liquid and gas media,
with no limitation on the relative size of the vortex core. The technique is then implemented to
estimate the translational velocity of a vortex ring in a Helmholtz vortex ring generator.

(Some figures in this article are in colour only in the electronic version)

1. Introduction and motivation

Squid, jellyfish and scallops belong to the diverse phylum
Mollusca. However, this is not their only similarity. These
marine animals are also jet-propelled swimmers. The
Cephalopoda, including squid, are a successful group of
the Mollusca and are related to bivalves such as scallops,
oysters and clams. Cephalopods, meaning 'head foot', are
characterized by a completely merged head and foot, with
a set of arms and/or tentacles surrounding the head. While
many of these molluscs, like the bivalves, do not have a head or
even a separate brain, cephalopods have well-developed senses
and large brains and are thought to be the most intelligent
of all invertebrates. They are also the most diverse of the
molluscs with more than 700 species to be found in all
of the world's oceans and in depths beyond 5 km. Two
groups of cephalopods exist today: the Nautiloidea with a few
species of the pearly nautilus, and the Coleoidea, containing
squid, cuttlefish, octopods and vampire squid. Cephalopods'
characteristic organs, the funnel and arms, are modifications of
the molluscan foot [1]. Living cephalopods are categorized by
the internal or external shells and number of tentacles; see [2].

Squid, like other cephalopods, use jet propulsion [3].
Squid are not only the fastest cephalopods but also the fastest
swimmers of all aquatic invertebrates. During swimming, their
long tapered bodies form an ideally streamlined configuration
while their lateral fins provide stability; see figure 1(a). The
swimming cycle starts with drawing water from the free edge
of the mantle and finishes with expelling it through a siphon,
or funnel, on the squid's underside. The length of the mantle
of a squid is covered by alternating rings of circular and radial
muscles, required for contraction of the cavity and respiration,
with connective tissue fibers in the muscle [4]. An opening in
the mantle cavity serves as an inhalant aperture, whereas the
funnel serves as the exhalent aperture. During the expulsion
cycle, the head is pulled back toward the body, sealing the
intake valves except the funnel. When the circular muscles
contract the cavity, the water is forced out of the funnel or
siphon. The flow of water can be controlled through a muscle
valve just inside the siphon's opening, allowing the jet to
be vectored in the appropriate direction. Using such a jet
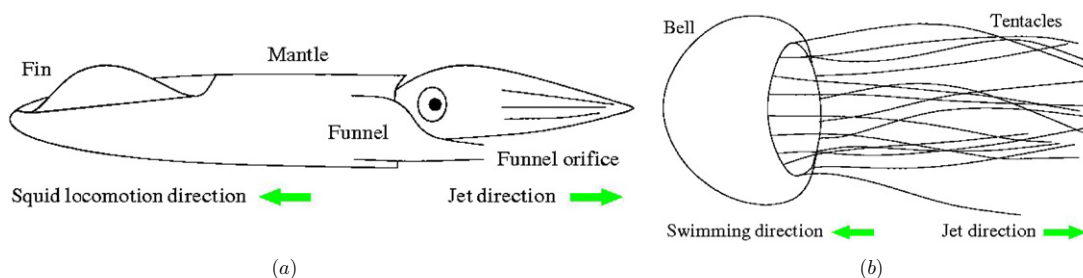
Figure 1. Jet-propelled marine animals: (a) Squid; (b) Jellyfish.
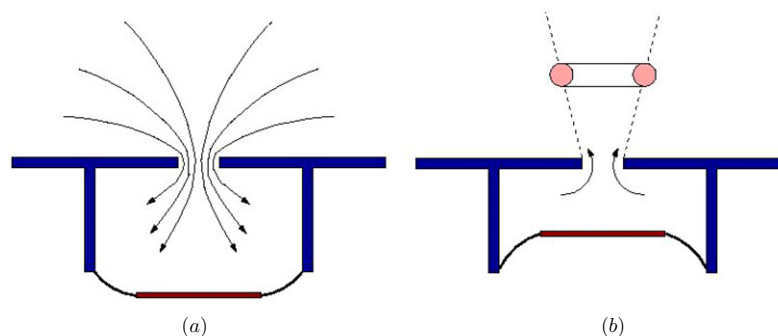
Figure 2. Vortex ring actuator concept: (a) fluid ingestion; (b) fluid expulsion and vortex ring formation.

propulsion technique, common Pacific squid can travel at 5–8 miles per hour (mph), while larger species have been recorded to move at around 20 mph. This suggests that pulsatile jets could be a viable locomotion technique for the design of underwater vehicles, as of yet unexplored in commercial vehicles.

Another example of jetting marine animals is jellyfish [5]. The body of a jellyfish consists of a bell-shaped membrane, enclosing its internal structure, with suspended tentacles; see figure 1(b). Most jellyfish are passive drifters that feed on plankton. As a result, low hydrodynamic drag and fast swimming speed are not important to them. That could explain their bluff hydrodynamic design. However, jetting and vortex formation is important to them for slow moving and creating water currents that collect and force food within reach of their tentacles. Jellyfish rely upon repeated contractions of an umbrella-shaped structure, or bell. During contraction, circular subumbrellar muscles pull the sides of the bell inward, reducing the volume of the subumbrellar cavity, and forcing water out through the velar aperture. Water is drawn back into the subumbrellar cavity during the relaxation phase. Because jellyfish are sensitive to light, limited vertical movement can also be important. The pulsating rhythm of the bell allows for some regulation of vertical movement and collection of food particles at the vortex core. The jellyfish can optimize its propulsion by controlling the diameter and velocity of the expelled jet at the exit of the velar aperture during vortex formation.

Motivated by squid jet propulsion, we have recently designed zero-mass flux vortex generators for low speed maneuvering of underwater vehicles [6–8]. Similar to squid or jellyfish, our actuator consists of a flexible cavity with an exit orifice. Through cyclic deflection of the diaphragm, low momentum fluid is ingested into the cavity and then expelled with a much higher momentum; see figure 2.

The initial structure of a starting jet is dominated by vortex ring formation [9, 10]. Periodic operation of a zero mass flux vortex generator results in the formation of a periodic array of vortex rings. A simple momentum balance analysis at the opening of such an actuator reveals that the net thrust generation depends on the wake structure and velocity of the generated vortex rings. To this end, this paper proposes a technique for estimating the speed of a vortex ring from the characteristics of the device that generate the vortex ring.

Most of the early experimental investigations on vortices were often limited to relatively thin vortices; see e.g., [9, 11, 12]. More recently, thicker vortices were investigated [10, 13]. Theoretical investigation on the translational velocity of a vortex ring is an old topic dating back to Kelvin [14] and Helmholtz [15]. Kelvin's result was extended to higher orders for the translational velocity of a *thin* axi-symmetric vortex ring in inviscid incompressible fluids; see e.g., [16–19]. All of these works are focused on relating the vortex velocity to the associated kinematic variables. In this investigation, however, we would like to extend these results to obtain the velocity of a *general* inviscid vortex from its intrinsic invariants of motion. Considering that in high Reynolds number vortex formation the flow invariants do not change during the vortex formation, one expects to calculate them from the characteristics of the vortex generator rather than the final vortices.

This paper is organized as follows. In the next section we will describe the morphology of a starting jet, in particular the formation of the leading vortex ring. Section 3 describes a bio-inspired vortex ring actuator that loosely mimics the
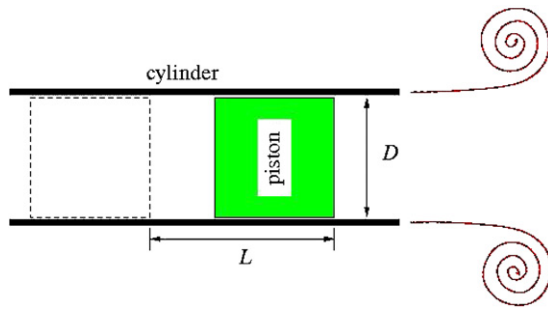
Figure 3. Piston-cylinder mechanism. D_r is the toroidal diameter of the vortex core. In Norbury notation this is $2l$.

propulsion of a squid. A general theory for estimating the translational velocity of a steadily moving vortical system is presented in section 4. Application of this formulation to vortex actuators is described in section 5. Finally our concluding remarks are presented in section 6.

2. Starting jets and vortex formation

The roll-up of an ejected shear layer from a nozzle or an orifice and the formation of vortex rings marks the initial phase of a starting jet. Vortex rings have captured the attention of many researchers over the last century. Vortex rings have relatively simple and persistent three-dimensional structure and at high Reynolds numbers they decay slowly. The generation, formation, evolution and interaction of vortex rings have been the subject of numerous investigations (see, e.g., Shariff and Leonard [20] and the references therein). This study is focused on estimating the speed of the resulting vortex in a starting jet from the characteristics of the actuator.

In a laboratory, vortex rings can be generated by the motion of a piston pushing a column of fluid through an orifice or nozzle; see figure 3. The boundary layer at the edge of the orifice or nozzle will separate and roll up into a vortex ring. The vortex ring has an induction velocity causing it to accelerate while the vortex ring grows. This combination of vortex ring enlargement and acceleration continues until the shear layer is unable to inject any more vorticity to the leading vortex ring. In this case the leading vortex ring is detached from the vortex sheet and the remaining vortex sheet becomes unstable and forms a trailing vortex ring. Continuation of this process in axi-symmetric flow will result in the formation of a periodic array of vortex rings.

The experiments of Gharib et al [10] have shown that for large piston stroke versus diameter ratio (L/D) in a piston-cylinder mechanism, the generated flow field consists of a leading vortex ring followed by a trailing jet. The vorticity field of the formed leading vortex ring is disconnected (pinched-off) from that of the trailing jet at a critical value of L/D (dubbed the 'formation number'), for which the vortex ring attains a maximum circulation. The formation number was in the range of 3.6 to 4.5 for a variety of exit diameters, exit plane geometries, and non-impulsive piston velocities.

Mohseni and Gharib [21] considered a relaxational model for the vortex ring pinch-off process, claiming that the

formation of vortex rings at relatively high Reynolds numbers is mainly an inviscid process. Therefore, the invariants of motion, namely the energy E, impulse I and circulation Γ must be the same initially and after the formation of vortex rings. Note that apart from the energy, impulse and circulation all the other invariants of motion (higher order vorticity moments) are lost during the mixing process and will not significantly affect the formation process [22]. The initial state was approximated by a fluid slug moving at a fixed velocity (piston velocity) and the final state was approximated by a vortex in the Norbury family of vortices [23]. They predicted an average formation number of 4 for the vortex ring pinch-off. It is important to note that the formation number of 4 is only achieved if the rates of generation of the integrals of motion are constant during the formation process. One can change the formation number by varying the rate that the invariants of motion are delivered to the system. It has been suggested [21, 24–28] that one can change the pinch-off formation number and consequently the size of the resulting vortex by varying: (*i*) the nozzle diameter or (*ii*) the speed of the shear layer (speed of the ejected fluid slug) during the formation process. Accelerating the shear layer results in a larger vortex ring while decelerating the shear layer results in a smaller vortex ring and consequently smaller critical formation number. This is verified numerically in high Reynolds number flows [24]. Note that these simulations also verified the assumption that the main invariants of motion in the pinch-off process are the kinetic energy, circulation and impulse and that the higher enstrophy densities did *not* play a significant role as long as the Reynolds number was relatively high [22]. Pulsation also has beneficial thrust augmentation. Krueger and Gharib [29] showed that the time-averaged thrust of an incompressible fully pulsed jet containing a period of no flow between pulses could be 90% higher than an un-pulsed jet. They traced back the origin of the thrust augmentation to vortex ring formation. All these observations point to a viable technique for thrust generation in underwater locomotion. A biomimetically inspired pulsatile jet actuator is described in the next section.

3. Biomimetic vortex actuators for locomotion of underwater vehicles

A major challenge in the design of autonomous underwater vehicles (AUVs) and remotely operated vehicles (ROVs) is maneuverability at low speeds. This is of particular importance during docking procedures. Inspired by the jet propulsion in cephalopods, described in section 1, we recently proposed a novel vortex ring generator for application in low speed maneuvering and propulsion of small underwater vehicles; see [6, 7, 30, 31].

Vortex ring jets can be generated using a variety of mechanical devices. While a squid generates vortex rings by muscle contraction around the mantle, we proposed a simple, yet effective mechanism for periodic vortex ring generation. To this end, prototypes of pulsatile jet vortex generators using the Helmholtz cavity concept (figure 4) were designed and built in our group. The jet propulsion of a squid is mimicked by the movement of a diaphragm wall of a cavity with an exit orifice.
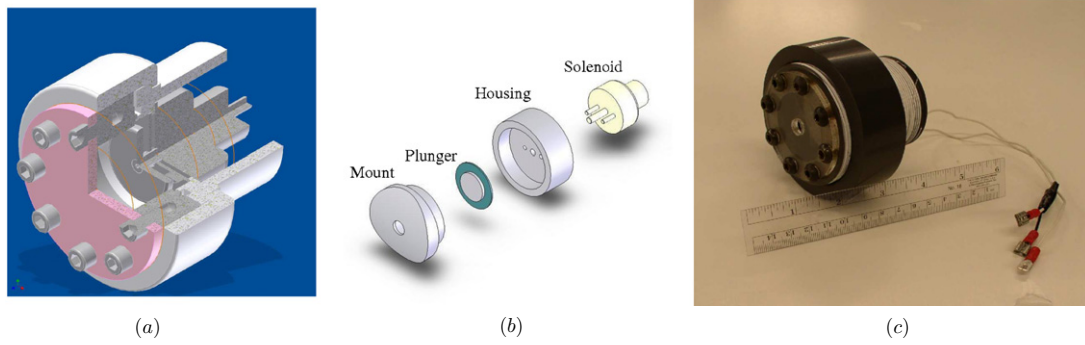
Figure 4. CU Boulder vortex ring actuator prototype: (a) CAD model of the actuator design; (b) plunger and solenoid assembly; (c) actual fabrication of the vortex ring actuator.
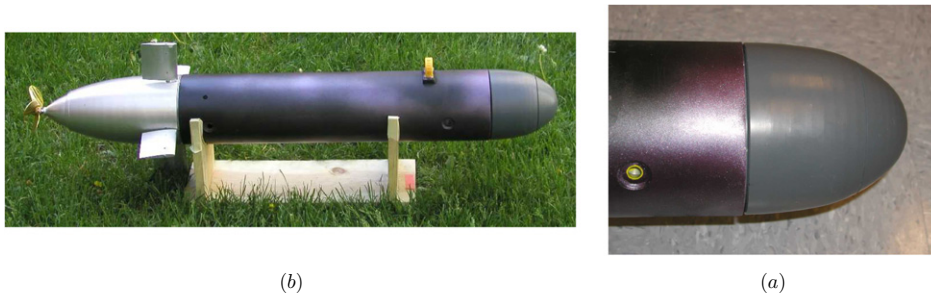
Figure 5. UUV test bed at the University of Colorado: (a) Colorado UUV; (c) exit nozzle of the SJA on the Colorado UUV.

Figure 4 shows the structure and appearance of a pulsatile jet actuator prototype. The driving diaphragm consists of a rigid disk with a flexible surround. Various actuation techniques can be employed for actuating the diaphragm. These include, but are not limited to, the use of solenoids, acoustic speakers, electrostatic and piezoelectric actuation. Currently a solenoid actuator is used to generate the diaphragm motion. In this design the inward movement of a diaphragm draws fluid into a chamber as depicted in figure 2(a). The subsequent outward diaphragm movement in figure 2(b) expels the fluid, forming a vortex ring or a jet depending on the formation number. Repetition of this cycle results in a pulsatile jet. Because of the asymmetry of the flow during the inflow and outflow phases, a net fluid impulse is generated in each cycle, even though there is no net mass flux through the chamber over one cycle. The experimental prototypes also allow easy substitution of different sized orifices and different sized chambers. In this way, physical parameters can be easily varied so that theoretical models can be compared against actual experimental results in different parameter regimes. This design has many advantages including its simplicity, few moving parts, and compactness. Figure 5 shows an unmanned underwater vehicle equipped with this technology. This vehicle served as a model test-bed for hybrid vehicle designs that combine pulsatile jets with conventional propellers and torpedo-like bodies. Note the proposed propulsion scheme has no protruding components that increase drag, has very few moving parts, and takes up relatively little volume. Such hybrid designs which incorporate both a main propeller and a distributed set of pulsatile jet actuators will improve low

speed underwater vehicle performance. While propellers clearly perform best at cruising speeds, pulsatile jets can significantly augment low speed maneuverability, and enable occasional loitering/hovering actions. Such pulsatile jets can also implement drag-reducing flow control (similar to what has been used in air and reported in [32]) while the vehicle is cruising under propeller power.

4. Translational velocity of a steady vortical system

The result of evolution of a pair of starting shear layers in two-dimensional and a shear tube in axi-symmetric flows are steadily translating vortices. In this section we derive an equation for the translational velocity of the resulting vortical system based on the overall parameters of the shear layer. To avoid lengthy calculations, we derive the formulae for the two-dimensional case. The axi-symmetric case can be derived similarly.

Consider a two-dimensional inviscid flow in unbounded regions. The equations of motion in stream function–vorticity (ψ–ω) are

$$\nabla^2 \psi = -\omega; \qquad (1)$$
$$\nabla \cdot \mathbf{u} = 0; \qquad (2)$$

where $\mathbf{u}$ is the velocity field. We are interested in flow states that are steady in some translating and rotating frame of reference with translational velocity (U, V) and rotational velocity Ω. In this system, the energy $E = \int \psi \omega \, dA$, linear impulses $I_x = \int \omega y \, dA$, and $I_y = - \int \omega x \, dA$, angular impulse $J = -\frac{1}{2} \int \omega r^2 \, dA$, and moments of the vorticity

$I_n = \int \omega^n \, dA$ are conserved. Kelvin stated that for isovortical perturbations the steady solutions of the two-dimensional and axi-symmetric inviscid flows are the extremum of

$$H = E - UI_x - VI_y - \Omega J, \qquad (3)$$

where U, V and Ω are the Lagrange multipliers [33]. In applications of interest in this paper we assume a zero angular impulse. Now, if one chooses x in the direction of the overall translational velocity, one can reduce this function to

$$H = E - UI, \qquad (4)$$

where I is the impulse in the translational velocity direction. This formulation is more suitable for our purposes. Now variation of H subject to isovortical perturbations and constraint I is

$$\delta H = \delta E - U \delta I = \int (\psi + Uy) \, \delta \omega \, dA. \qquad (5)$$

Note that $\delta E = \int \psi \delta \omega \, dA$. For area preserving perturbations one can show that [34]

$$\delta \omega = -\frac{\partial e}{\partial y} \frac{\partial \omega}{\partial x} + \frac{\partial e}{\partial x} \frac{\partial \omega}{\partial y} \qquad (6)$$

for an arbitrary function e. Hence, integrating by parts results in

$$\delta H = \int \left(\left(\frac{\partial \psi}{\partial y} + U \right) \frac{\partial \omega}{\partial x} - \frac{\partial \psi}{\partial x} \frac{\partial \omega}{\partial y} \right) e \, dA. \qquad (7)$$

For a steady case $\delta H = 0$. Now in a frame of reference moving with velocity U, equation (7) reduces to

$$\frac{\partial \psi}{\partial y} \frac{\partial \omega}{\partial x} - \frac{\partial \psi}{\partial x} \frac{\partial \omega}{\partial y} = 0, \qquad (8)$$

which is exactly the equation of motion. Consequently, the equation of motion for steady inviscid flow is an extremum of function H. In other words, the two-dimensional steady Euler equation and the variational approach presented by the equation $\delta H = 0$ are equivalent. This provides the context for an equation for the translational velocity of a steadily moving vortical system based on equation (5). That is

$$U = \left. \frac{\delta E}{\delta I} \right|_{\text{for isovortical perturbations.}} \qquad (9)$$

In the case of simplified vortex distribution, such as uniform vorticity density distribution in Norbury vortices, the isovortical perturbations could be limited to constant vortex volume and circulation.

A similar calculation for axi-symmetric flows, not repeated here, results in similar formulae for the translational velocity. It should be pointed out that the same equation for thin axi-symmetric vortex rings was also proposed by Robert and Donnelly [17, 35] using a different derivation. Here, this result was extended to a more general set of vortices.

The challenge is now to calculate the variational derivative of kinetic energy with respect to impulse for isovortical perturbations for any vortex generators. For this reason it is of great importance to know the rate of generation of invariants of motion for a particular vortex generator. In fact, we believe that to a first-order approximation a vortex generator can be characterized by the rate of creation of kinetic energy, impulse and circulation. This will become evident in the next section when an estimate for the translational velocity of a vortex ring at the exit of a nozzle in actuators described in section 3 is presented.
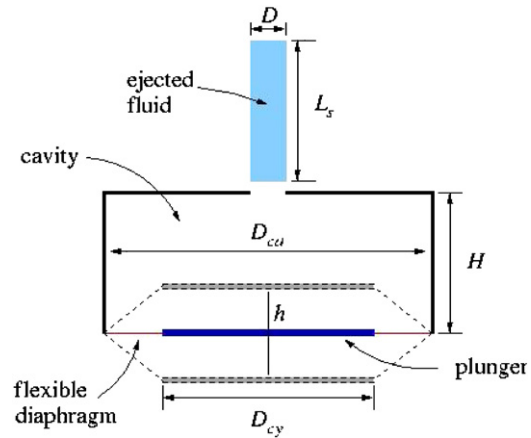

Figure 6. Actuation of a zero mass flux vortex actuator.

5. Translational velocity of an axi-symmetric shear tube

There are various experimental and numerical methods to generate vortex rings. Each of them generates invariants of motion at a particular rate. In order to predict the translational velocity of the ejected vortical system for each vortex generator one needs to estimate the rate of injection of invariants of motion for that particular vortex ring generator.

Consider an arbitrary generator of axi-symmetric vortex sheets. A popular example is a piston-cylinder mechanism, where a cylindrical shear layer is ejected from the exit of a cylinder at a particular speed, approximately the piston velocity[1] U_p (see figure 3). This is similar to ejection of a fluid slug from a vortex generator as depicted in figure 6. Note that the length of the ejected slug in this actuator can be calculated by equating the volume of the ejected fluid slug to the total volume change due to the movement of the flexible diaphragm.

As described in section 2, the flow field of an impulsively started jet consists of a leading vortex ring followed, if the piston stroke versus diameter ratio is large, by a trailing jet. In order to model this process we use the technique proposed in [22]. We approximate the initial state by a column of fluid with diameter $D = 2R$ and length L moving at a constant velocity U_p (piston velocity) and the final state is approximated by a vortex in the Norbury family of vortices. The slug model is characterized by the following relations for the energy, circulation and impulse of the ejected fluid:

$$E = \frac{1}{8} \pi D^2 L U_p^2 = \frac{I \Gamma}{L} \qquad (10)$$

$$\Gamma = \frac{L U_p}{2} = \frac{I}{2 \pi R^2} \qquad (11)$$

$$I = \frac{1}{4} \pi D^2 L U_p = \frac{1}{2} \pi D^2 \Gamma. \qquad (12)$$

---

[1] We assumed that the jet velocity is approximately U_p, but for jets ejected through an orifice the jet velocity may be substantially higher than U_p due to jet contraction past the jet exit plane. These effects are not considered here.
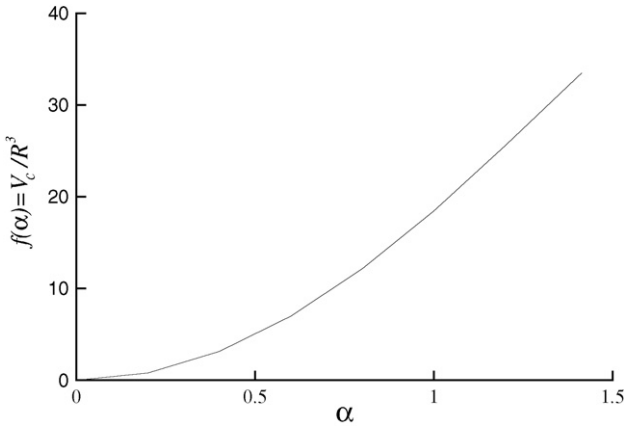
Figure 7. Volume of core in Norbury vortices.

The slug model provides an estimate of the invariants of motion initially injected into the medium. On the other hand, we assume that the invariants of motion after the formation can be estimated by the invariants of motion for a vortex in the Norbury family of vortices.

5.1. Translational velocity of a vortex ring

Velocity of a steadily translating axi-symmetric vortex is a constant of motion in inviscid flows. Theoretical prediction of translational velocity of thick vortex rings is a challenging task. Translational velocity depends on the rate at which the invariants of motion are provided to the system. In the slug model we can estimate the translational velocity from equation (9),

$$U_{tr} = \left. \frac{\delta E}{\delta I} \right|_{\text{constant } \Gamma \text{ and vortex volume}}. \tag{13}$$

Considering zero variation in the vortex ring circulation, equation (10) yields

$$\frac{\delta E}{\delta I} = \frac{\Gamma}{L} - \frac{E}{L}\frac{\delta L}{\delta I} = \frac{U_p}{2} - \frac{E}{L}\frac{\delta L}{\delta I}. \tag{14}$$
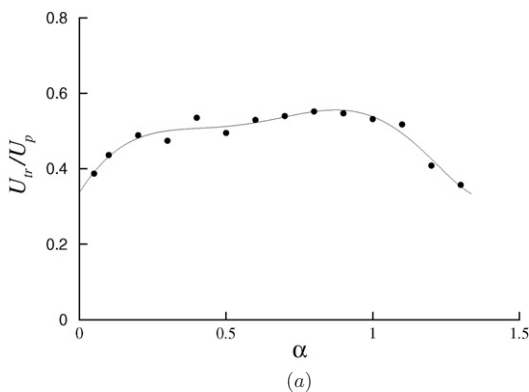
To simplify the variational derivative on the right-hand side of equation (14), one can employ equations (11) and (12) for the impulse to calculate

$$\delta I = \frac{2I}{R}\delta R. \tag{15}$$

By substituting δI into equations (14) one obtains

$$\frac{\delta E}{\delta I} = \frac{U_p}{2} - \frac{ER}{2LI}\frac{\delta L}{\delta R}. \tag{16}$$

In order to proceed we employ Norbury's result to calculate $\frac{\delta L}{\delta R}$. Norbury vortices are steady solutions of Euler equations with one parameter α, non-dimensional mean core radius. The vorticity density distribution $\Omega = \omega/r$ is constant in each vortex. Norbury vortices range from vortex rings of small cross section as α approaches zero to Hill's spherical vortex for $\alpha = \sqrt{2}$. Using the non-dimensionalization employed by Norbury one can write

$$E = (\Omega\alpha^2 l^2)^2 E_N; \tag{17}$$
$$\Gamma = (\Omega\alpha^2 l^2)l\Gamma_N; \tag{18}$$
$$I = (\Omega\alpha^2 l^2)l^3 I_N; \tag{19}$$

where the subscript N indicates the corresponding non-dimensional quantity for a Norbury vortex. Here, l is the vortex radius [23].

By equating the non-dimensional impulse from the slug model with the same quantity calculated from the Norbury family of vortices one obtains

$$\frac{L}{D} = \sqrt{\frac{\pi}{2}}\frac{I_N^{1/2}\Gamma^{3/2}}{E_N} = g(\alpha). \tag{20}$$

We assumed that $D \approx 2l$. Note that the right-hand side of equation (20) is a function of α only. Here we derive an explicit formula for the translational velocity of a vortex ring with a mean core radius of α.

From equation (20) one obtains

$$\frac{\delta L}{\delta R} = \frac{L}{R} + 2g'(\alpha)R\frac{\delta\alpha}{\delta R}. \tag{21}$$

The constraint on the volume of the vortex ring is employed to derive an equation for $\delta\alpha/\delta R$. Norbury [23] provided results
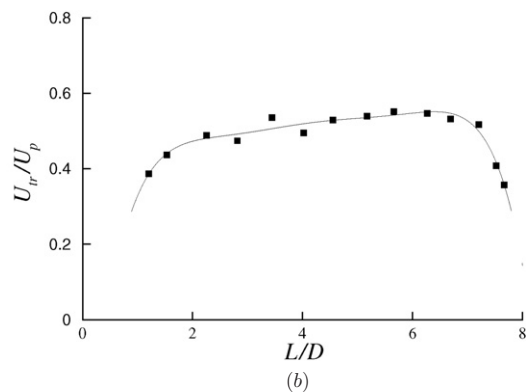
Figure 8. Variation of the translation velocity of a vortex ring (in slug model—Norbury vortices) with (a) the mean core radius, and (b) formation number L/D. Circles are the data points and the solid line is the curve fitted data points.

for the vortex ring volume as a function of the mean core radius, namely $V_c = f(\alpha) R^3$. $f(\alpha)$, produced in figure 7, is a function of the mean core radius α only. Hence

$$R \frac{\delta\alpha}{\delta R} = -3 \frac{f(\alpha)}{f'(\alpha)}. \tag{22}$$

Now equation (21) can be recast as

$$\frac{R}{L} \frac{\delta L}{\delta R} = 1 - 3 \frac{g'(\alpha)}{g(\alpha)} \frac{f(\alpha)}{f'(\alpha)}. \tag{23}$$

Finally, the translational velocity in equations (13) and (14) can be written as

$$\frac{U_{tr}}{U_p} = \frac{1}{4} \left(1 + 3 \frac{g'(\alpha)}{g(\alpha)} \frac{f(\alpha)}{f'(\alpha)} \right). \tag{24}$$

This function is depicted in figure 8 using Norbury's data [23]. There are slight fluctuations in this graph, which is a consequence of calculating derivatives from relatively coarse data from Norbury [23]. For most values of the mean core radius, particularly for $2 \lesssim L/D \lesssim 5$ the slug model predicts a translational velocity around $U_p/2$ with slight velocity increase as the formation number increases. This is consistent with a previous assumption in [21]. At higher values of α which corresponds to larger formation number L/D in the slug model there is a significant drop in the translational velocity. This is a limitation of the slug model which assumes that the relative rate of injecting invariants of motion is constant and not dependent on the formation number. However, in reality, the formation and growth of boundary layers at the orifice walls will change the effective velocity and diameter of the ejecting fluid [26]. It is expected that inclusion of such effects results in better prediction of the translational velocity for larger formation numbers. In general, the slug model is not a good representation of the invariants of motion for very large or very small formation numbers.

6. Conclusions

A technique for calculating the translational velocity of a steady vortical structure is derived. The technique uses the critical point of a functional defined based on the invariants of motion during the formation process. This technique was employed for estimating the translational velocity of a vortex ring ejected from a zero mass flux vortex generator. The particular vortex generator investigated is designed to mimic the jet propulsion of cephalopods. An equation for the translational velocity of a vortex ring is derived from a combination of the slug model and Norbury vortices. The resulting velocity is a function of the mean core radius α of the vortex or the formation number L/D. The same technique could potentially be used to estimate the speed of a vortex ring (for axi-symmetric flows) and a vortex pair (for two-dimensional flows) in other vortex generators. Future work involves accommodation for an improved slug model such as circulation correction by Krueger [36] and effects of the boundary-layer growth on the jet centerline velocity [26, 37]. Although this paper is mostly focused on application of the theory to pulsatile jets, it should be noted that similar calculations can be conducted to connect the vortex theory of animal flight to its wake structure and wing kinematics. This will be the topic of a future investigation.

References

[1] Lehmann U and Hilmer G 1983 *Fossil Invertebrates* (Cambridge: Cambridge University Press)
[2] Pojeta J 1987 Phylum mollusca *Fossil Invertebrates* ed R S Boardman, A H Cheetham and A J Rowell (Palo Alto, CA: Blackwell Scientific Publishing)
[3] Anderson E J and DeMont E 2000 The mechanics of locomotion in the squid *loligo pealei*: locomotory function and unsteady hydrodynamics of the jet and intramantle pressure *J. Exp. Biol.* **203** 2851–63
[4] Ward D V 1972 Locomotory aspects of squid mantle structure *J. Zool.* **167** 437–49
[5] DeMont E and Gosline J 1988 Mechanics of jet propulsion in the hydromedusan jellyfish, polyorchis penicillatus *J. Exp. Biol.* **134** 347–61
[6] Mohseni K 2004 Pulsatile jets for unmanned underwater maneuvering *3rd AIAA Unmanned Unlimited Technical Conference, Workshop and Exhibit (Chicago, IL, 20–23 September 2004)* (AIAA paper 2004-6386)
[7] Mohseni K 2006 Pulsatile vortex generators for low-speed maneuvering of small underwater vehicles *Ocean Eng.* **33** 2209–23
[8] Krieg M, Pitty A, Salehi M and Mohseni K Optimal thrust characteristics of a synthetic jet actuator for application in low speed maneuvering of underwater vehicles *Proceedings of the OCEANS 2005 (Washington, DC, 19–23 September 2005)* MTS/IEEE
[9] Glezer A 1988 The formation of vortex rings *Phys. Fluids* **31** 3532–42
[10] Gharib M, Rambod E and Shariff K 1998 A universal time scale for vortex ring formation *J. Fluid Mech.* **360** 121–40
[11] Maxworthy T 1977 Some experimental studies of vortex rings *J. Fluid Mech.* **80** 465–95
[12] Auerbach 1987 Experiments on the trajectory and circulation of the starting vortex *J. Fluid Mech.* **183** 185–98
[13] Dabiri J O and Gharib M 2004 Fluid entrainment by isolated vortex rings *J. Fluid Mech.* **511** 311–31
[14] Kelvin Lord 1867 The translatory velocity of a circular vortex ring *Phil. Mag.* **4** 511–2
[15] Helmholtz H 1867 On integrals of hydrodynamical equations which express vortex-motion *Phil. Mag.* **4** 485–512
[16] Dyson F W 1893 The potential of an anchor ring: part II. *Phil. Trans. R. Soc.* A **184** 1041–106
[17] Robert P H and Donnelly R J 1970 Dynamics of vortex rings *Phys. Lett.* **31** 137–8
[18] Fraenkel L E 1972 Examples of steady vortex rings of small cross-section in an ideal fluid *J. Fluid Mech.* **51** 119–35
[19] Moffatt H K and Fukumoto Y 2000 Motion and expansion of a viscous vortex ring: part I. A higher-order asymptotic formula for the velocity *J. Fluid Mech.* **417** 1–45
[20] Shariff K and Leonard A 1992 Vortex rings *Ann. Rev. Fluid Mech.* **34** 235–79
[21] Mohseni K and Gharib M 1998 A model for universal time scale of vortex ring formation *Phys. Fluids* **10** 2436–8
[22] Mohseni K 2001 Statistical equilibrium theory of axisymmetric flows: Kelvin's variational principle and an explanation for the vortex ring pinch-off process *Phys. Fluids* **13** 1924–31

[23] Norbury J 1973 A family of steady vortex rings *J. Fluid Mech.* **57** 417–31

[24] Mohseni K, Ran H and Colonius T 2001 Numerical experiments on vortex ring formation *J. Fluid Mech.* **430** 267–82

[25] Mohseni K 2004 Studies of two-dimensional vortex streets *31st AIAA Fluid Dynamics Conference and Exhibit (Anaheim, CA, June 2001)* (AIAA paper 2001-2842)

[26] Shusser M, Gharib M, Rosenfeld M and Mohseni K 2002 On the effect of pipe boundary layer growth on the formation of a laminar vortex ring generated by a piston/cylinder arrangement *Theor. Comp. Fluid Dyn.* **15** 303–16

[27] Shusser M and Gharib M 2000 Energy and velocity of a forming vortex ring *Phys. Fluids* **12** 618–21

[28] Dabiri J O and Gharib M 2005 Starting flow through nozzles with temporally variable exit diameter *Phys. Fluids* **538** 111–36

[29] Krueger P S and Gharib M 2005 Thrust augmentation and vortex ring evolution in a fully pulsed jet *AIAA J.* **43** 792–801

[30] Krieg M, Coley C, Hart C and Mohseni K Synthetic jet thrust optimization for application in underwater vehicles *Proc. 14th Int. Symp. on Unmanned Untethered Submersible Technology (UUST) (Durham, NH, 21–24 August 2005)*

[31] Frost Gorder P 2004 Search for the perfect vortex: vortex drive *New Sci.* **184** 30–4

[32] Glezer A and Amitay M 2002 Synthetic jets *Ann. Rev. Fluid Mech.* **34** 503–29

[33] Lord Kelvin 1910 *Mathematical and Physical Papers* vol 4 (Cambridge: Cambridge University Press)

[34] Saffman P G 1992 *Vortex Dynamics* (Cambridge: Cambridge University Press)

[35] Robert P H 1972 A Hamiltonian theory for weakly interacting vortices *Mathematika* **19** 169–79

[36] Krueger P S 2005 An over-pressure correction to the slug model for vortex ring circulation *J. Fluid Mech.* **545** 427–43

[37] Dabiri J O and Gharib M 2004 A revised slug model boundary layer correction for starting jet vorticity flux *Theor. Comput. Fluid Dyn.* **17** 293–5